Nuclear Engineering and Technology 54 (2022) 3293–3298

Contents lists available at ScienceDirect

Nuclear Engineering and Technology

journal homepage: www.elsevier.com/locate/net

Original Article

Surface removal of stainless steel using a single-mode continuous wave fiber laser to decontaminate primary circuits

Ki-Hee Song, Jae Sung Shin*

Korea Atomic Energy Research Institute, 111, Daedeok-daero 989beon-gil, Yuseong-gu, Daejeon, 34057, Republic of Korea

ARTICLE INFO

Article history:
Received 13 January 2022
Received in revised form
28 March 2022
Accepted 28 March 2022
Available online 5 April 2022

Keywords:
Laser decontamination
Laser cleaning
Nuclear decommissioning
Primary circuits

ABSTRACT

Removing radioactive contaminated metal materials is a vital task during the decommissioning of nuclear power plants to reduce the cost of the post-dismantling process. The laser decontamination technique has been recognized as a key tool for a successful dismantling process as it enables a remote operation in radioactive facilities. It also minimizes exposure of workers to hazardous materials and reduces secondary waste, increasing the environmental friendliness of the post-dismantling processing. In this work, we present a thorough and efficient laser decontamination approach using a single-mode continuous-wave (CW) laser. We subjected stainless steels to a surface-removal process that repetitively exposes the laser to a confined region of ~75 μm at a high scanning rate of 10 m/s. We evaluate the decontamination performance by measuring the removal depth with a 3D scanning microscope and further investigate optimal removal conditions given practical parameters such as the laser power and scan properties. We successfully removed the metal surface to a depth of more than 40 μm with laser power of 300 W and ten scans, showing the potential to achieve an extremely high DF more than 1000 by simply increasing the number of scans and the laser power for the decontamination of primary circuits.

1. Introduction

The laser decontamination technique has been recognized as a very powerful tool with which to decontaminate radioactive contaminated metal materials in dismantling of a nuclear power plant. This method enables remote operation with automated systems in radioactive facilities, resulting in minimal exposure of workers to hazardous materials. Moreover, it offers reliable decontamination performance of metals with minimal modification of the surface properties while also reducing secondary waste from the decontamination process, meaning that it is a cost-effective and environmentally friendly post-dismantling process.

The primary circuits in nuclear power plants are contaminated with radioactive isotopes (RIs) due to several mechanisms, such as van der Waals's interaction and chemical trapping [1,2]. The material of the primary circuit components is typically austenite stainless steel [3]. Its surface is covered with an outer oxide layer typically with a depth of ~10 μm, and the base alloy contains several types of compounds, such as Fe, Cr, and Ni at depth in a range of 5–30 μm [4,5]. RI contaminants are mostly deposited inside the oxide layer and can be removed with a soft decontamination method, offering a decontamination factor (DF) of typically < 50 by solely removing the oxide layer [4]. Here, the decontamination factor is defined by Ref. [5]:

$$\mathrm{DF}=\frac{\text{Contamination level of substrate before the decontamination}}{\text{Contamination level of substrate after the decontamination}}$$

Thus, the percentage of removed contamination can be expressed by:

$$\text{Contamination removed }(\%)=\left(1-\frac{1}{\mathrm{DF}}\right)\times 100$$

However, RI compounds can penetrate into a deeper layer beyond the oxide layer due to stress corrosion cracking [3]. Thus, for thorough decontamination, which typically requires a DF exceeding 50, the metal base substrate should be removed to a depth of more than 40 μm after the removal of the oxide layer [4].

This task has been tackled by several laser decontamination techniques [6–15]. Industrial applications of laser techniques, such as laser cleaning and laser marking, require relatively a low power density level (typically < kW/cm^2), whereas nuclear applications

* Corresponding author.
E-mail address: jsshin12@kaeri.re.kr (J.S. Shin).

https://doi.org/10.1016/j.net.2022.03.040

including laser decontamination and laser decommissioning techniques require an extremely high power density level, with a range of tens of kW/cm^2 to the MW/cm^2 scale. This emphasizes the necessity of the proper selection of a reliable high-power fiber laser and its delicate operation for successful laser decontamination of metals. A high-power multi-mode and diode lasers have gained significant attentions for the laser decontamination of metals due to its stable reliability and cost-effectiveness. In particular, Minehara and Tamura demonstrated the feasibility of laser decontamination for removing RI-contaminated materials using a single-mode continuous wave (CW) laser, as it provides a good beam quality and a tiny focal spot size, permitting the thorough and efficient decontamination of metals via a cost-effective method [11,12]. They performed laser decontamination of heavily RI-contaminated stainless-steel samples in the primary cooling loop of a nuclear power reactor, obtaining the DF of 3300 in average and a few below the detection limit [12]. Nonetheless, the effects of various experimental conditions on the surface-removal performance outcomes for single-mode CW laser-based decontamination have not yet been thoroughly reported.

In this work, we not only perform the surface removal of stainless steels using a single-mode CW laser but also investigate the optimal removal conditions given certain practical parameters, in this case the laser power, scanning speed, scan step size, and number of scans. Specifically, we present the feasibility of decontaminating stainless steels by exposing confined areas of these materials to very high power levels over short periods of time. In other words, by scanning with the single-mode CW laser using a very small focal spot size of ~75 μm rapidly and repeatedly, we minimize the intrinsic melting issue that may occur during the decontamination process. In addition, we evaluate the decontamination performance by measuring the removal depth via three-dimensional (3D) scanning microscope and further investigate the effects of the scanning properties on the removal depth.

2. Methods

Fig. 1(a) shows a schematic of the laser decontamination system, which consists of a 1080-nm fiber laser (RFL-C1000, Raycus), a pair of galvanometer scanning mirrors (S9210, Sunny Technology), and a *f*-theta lens. The fiber laser is a 1-kW single-mode CW laser with a core size of 25 μm and beam quality of 1.3, which enables us to focus light within a very small focal spot area. Although the laser can generate output power up to 1000 W, the laser power was limited to approximately 300 W to avoid damage to the scanning mirrors. The laser output beam was collimated by a collimator (f = 50 mm), guided by the two galvanometer scanning mirrors, and focused by the *f*-theta lens (f = 160 mm) onto the sample with a focal spot size of ~75 μm and average power density of ~3.4 MW/cm^2. We used compressed air as the assist gas to blow out the dust as shown in Fig. 1(a). The extraction and filtration (E&F) system was installed near the sample to collect any debris generated during the laser decontamination process, as shown in Fig. 1(b).

We prepared a stainless-steel sample of SUS304, which is a common material used in the primary circuits of nuclear power plants [3], to demonstrate the laser decontamination system. The sample size is 120 mm × 75 mm × 100 mm.

We adjusted the scan pattern using a customized CS-mark software (CS-mark, Sunny Technology) and scanned the laser in a rectangular zigzag pattern, as shown in Fig. 1(c). Fig. 2(a) and (b) show photos taken during the laser decontamination process using an actual sample and a sample treated by laser decontamination as described here, respectively.

3. Results

3.1. Influence of the scan properties on the removal surface

Certain scan properties, such as the scan step size and scan speed, are key considerations when decontaminating metals, as they influence the surface texture of the laser decontamination substrate [8]. It is well known that exposure durations of more than several milliseconds can damage the surface due to the melting of the metal [15–17]. This leads to the penetration of RI contaminants deep inside the metal bulk by shallow fusion or oxidation [18]. Also, a sparse spacing between consecutive scanning events may cause an inefficient exposure over the decontaminating area [6]. Thus, it is critical to determine the optimal scanning conditions for successful laser decontamination. Accordingly, we initially tested the influence of the scan step size on the removal surface at a fixed laser power of 301 W and scan speed of 10 m/s. The number of scans was set to ten for this experiment.

Fig. 3 shows photos of four treated samples with different scan step size values (from 1.15 mm to 11.5 μm). We observed irregular patterns along the scanning path in most cases (Fig. 3(a–c)) whereas we observed a quite uniform surface morphology over the entire decontaminating area when the step size was 11.5 μm (Fig. 3(d)). Notably, the 57.5-μm step size case (Fig. 3(c)) failed to decontaminate the sample efficiently along the scanning path, despite the fact that its scan step size corresponds to the measured focal spot size (75 μm). The observed irregular patterns provide a clue by which to trace the exposure morphology during the scan, indicating that the scan step size should be small enough relative to the focal spot size to obtain an even surface morphology. Thus, we used a scan step size of 11.5 μm in the subsequent experiments.

Next, in order to ascertain the optimal exposure conditions of the CW laser onto the metal surface, we tested the influence of the scan speed, which is one of the key parameters when determining the total delivered energy per unit surface area and subsequently the decontamination performance [6], on the removal depth at a fixed scan step size of 11.5 μm and fixed laser power of 301 W. The number of scans was set to two to minimize the accumulated laser fluence and for a clear observation of the surface morphology. Fig. 4 shows photos of five treated samples at different scan speeds (from 15 m/s to 1 m/s). The surface starts to show an uneven texture at a scan speed of 5 m/s, as shown in Fig. 4(c–e), and clearly shows non-uniformly aggregated areas at a scan speed of 1 m/s. These aggregated textures may cause RI compounds to accumulate in the inner layers and lower the DI. Thus, the scan speed must be fast enough to minimize damage to the surface of the metals, especially when using a CW laser. Here, we selected a scan speed of 10 m/s in the subsequent experiments.

3.2. Influence of the number of scans on the removal depth

Using the scan conditions selected above, we investigated the influence of the number of scans on the removal depth with a fixed laser power of 300 W and fixed scan speed of 10 m/s. The number of scans was varied from 3 to 20, as shown in Fig. 5(a). We measured the removal depth after laser decontamination using a laser scanning microscope (VHX5000, Keyence), which provides the height profile and surface morphology of the treated sample after undergoing laser decontamination [8]. In order to measure the removal depth, we initially selected the region of interest (ROI) of the treated sample, as indicated by the blue solid box in Fig. 5(b), and captured a 3D image of the ROI via laser scanning microscope. Fig. 5(c) shows a two-dimensional (2D) projection image of the acquired 3D image. Then, we extracted the profile from the center line of the 2D image, as described in Fig. 5(d). We measured the

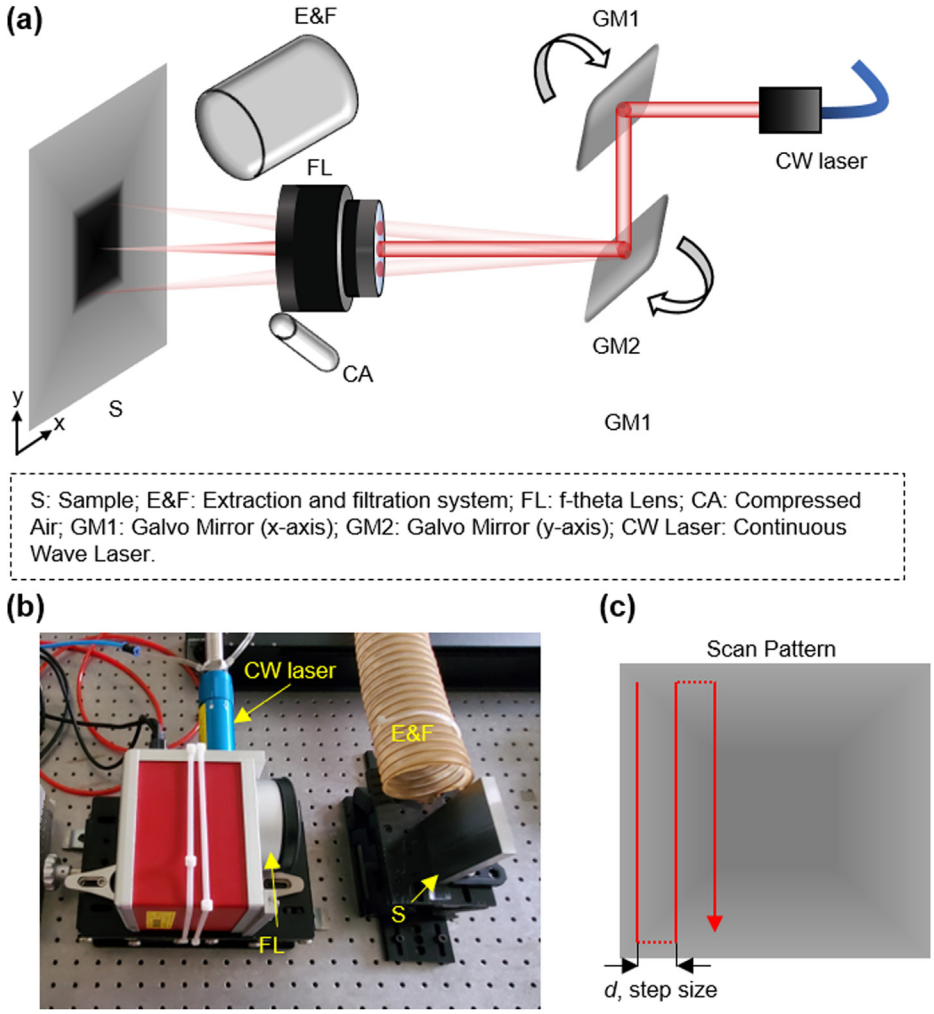

Fig. 1. Laser decontamination system (a) Schematic of the experimental setup. (b) Photo of the experimental setup. (c) Scan pattern used in the experiment.

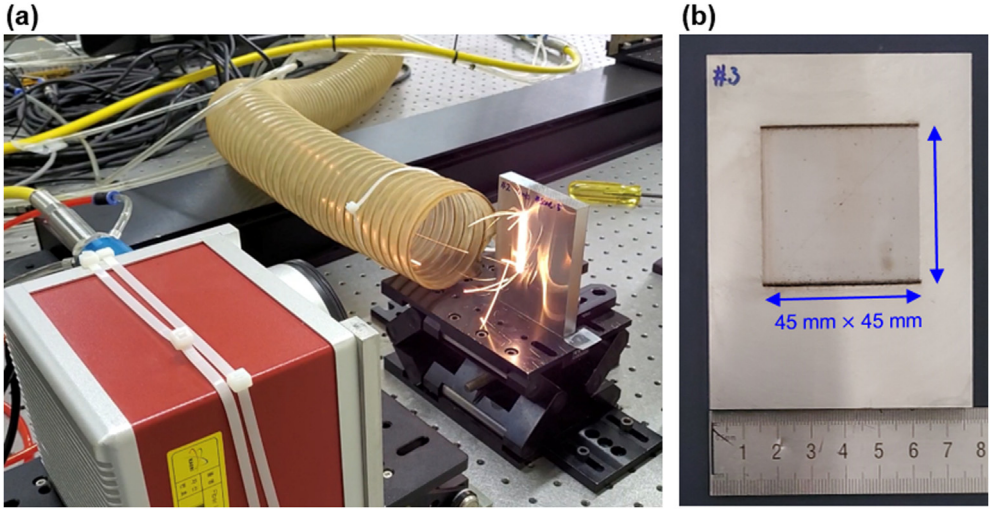

Fig. 2. Laser decontamination experiment (a) Photo of the laser decontamination process. (b) Photo of a treated sample by laser decontamination. The scan area is 45 mm × 45 mm.

differences between the treated and untreated regions (blue solid boxes in Fig. 5(d); 30 μm length per region). We defined the average value as the removal depth in all experiments.

As shown in Fig. 5(a), the removal depth of the stainless steel here increases constantly with an increase in the number of scans. Fig. 5(b) shows a photo of the treated sample when the number of scans was set to 3, achieving a removal depth of ~1.5 μm. We achieved a removal depth of ~42 μm when the number of scans was

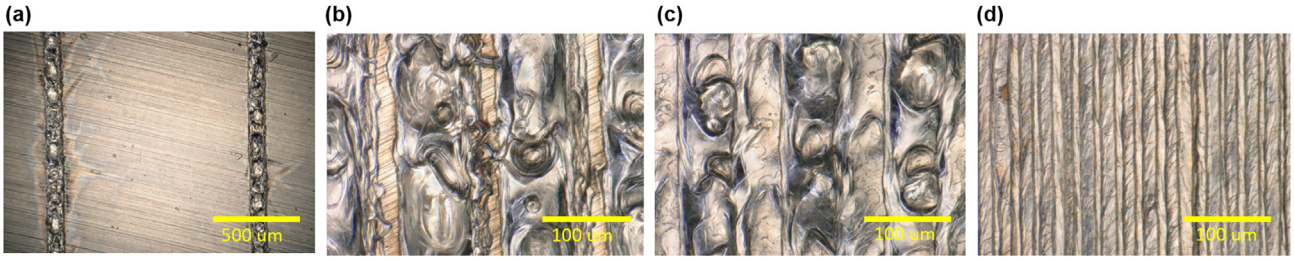

Fig. 3. Influence of the scan step size on the removal shape. Images of surfaces of treated samples when the scan step size values are (a) 1.15 mm, (b), 115 μm, (c) 57.5 μm, and (d) 11.5 μm.

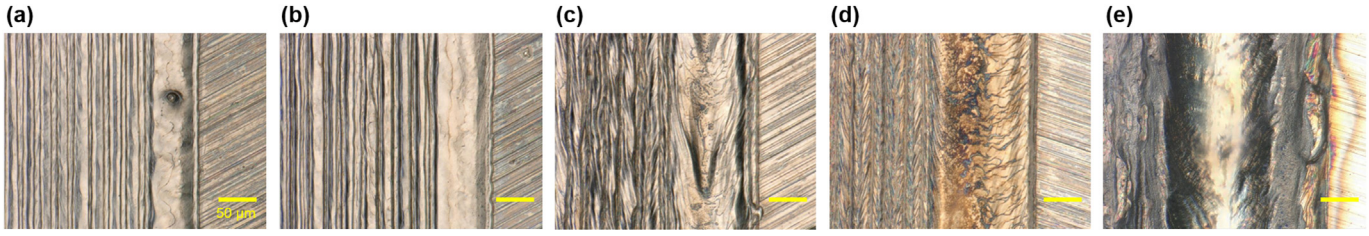

Fig. 4. Influence of the scan speed on the removal shape. Images of the surfaces of treated samples at (a) 15 m/s, (b) 10 m/s, (c) 5 m/s, (d) 3 m/s, and (e) 1 m/s.

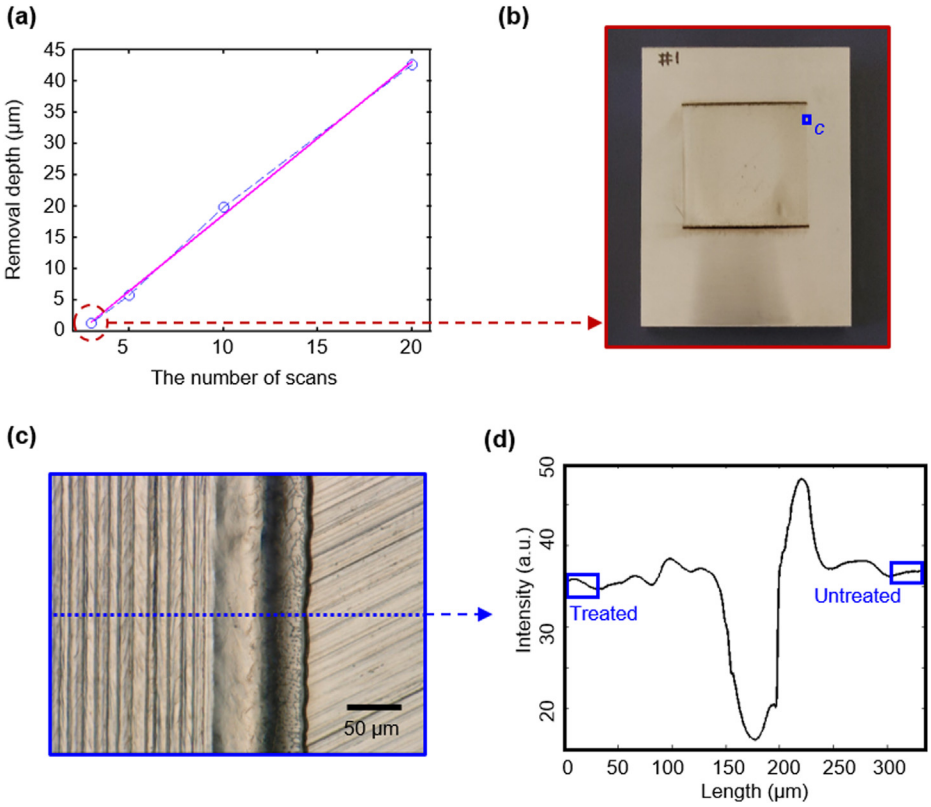

Fig. 5. Influence of the number of scans on the removal depth (a) Removal depth as a function of the number of scans (b) Photo of a sample treated by laser decontamination (c) 2D projection image of the blue inset box in (b). (d) Profile of the center line in Fig. 2(c). Note that the size of the blue inset box in Fig. 2(b) is exaggerated here for better visualization. A length of 30 μm was used to estimate the depth removal of treated and untreated regions. (For interpretation of the references to colour in this figure legend, the reader is referred to the Web version of this article.)

set to 20, which is enough to achieve a DF exceeding 100 [4]. It was evident that the removal depth was proportional to the number of scans, implying that the removal depth could be deeper as the number of scans is increased. This result confirmed the feasibility of the laser decontamination of metals using a single-mode CW laser and further paves the way for achieving an extremely high DF up to 10000 by simply controlling the number of scans during the actual dismantling process.

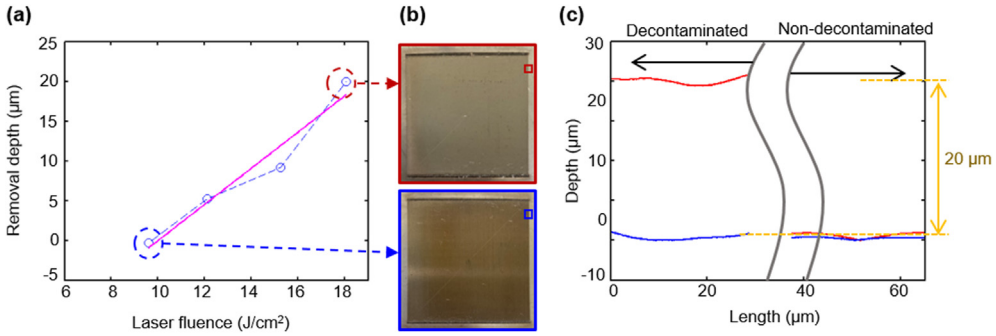

Fig. 6. Influence of the laser fluence on the removal depth (a) Removal depth as a function of the laser fluence (b) Images of a sample treated at fluence levels of 18 J/cm^2 (top red box) and 7 J/cm^2 (bottom green box). (c) Corresponding profiles of treated and untreated regions in samples. (For interpretation of the references to colour in this figure legend, the reader is referred to the Web version of this article.)

3.3. *Influence of the laser fluence on the removal depth*

Laser decontamination is based on the laser ablation phenomenon, referring to the accumulative process that occurs when light energy is absorbed in a very short period of time in a confined area. The absorbed energy is rapidly converted to heat and subsequently evaporates solid materials, leading to the removal of contaminants from substrate surfaces [9]. The efficiency of laser ablation is predominantly determined by the laser fluence, together with the wavelength, material properties, and scan properties, and can be evaluated using the removal depth [8]. Accordingly, we investigated the influence of the laser fluence on the removal depth at a fixed scan speed and fixed number of scans. We changed the laser fluence levels of 7 J/cm^2 and 18 J/cm^2. The number of scans and the scan speed were set to 10 and 10 m/s, respectively, for this experiment.

Fig. 6(a) shows the removal depth as a function of the laser fluence. Overall, the removal depth increases when increasing the laser fluence. Fig. 6(b) shows images of a sample treated at fluence levels of 18 J/cm^2 (top red box) and 7 J/cm^2 (bottom green box), and Fig. 6(c) shows the corresponding profiles of treated and untreated regions in samples. Notably, we found that the ablation threshold level is ~10 J/cm^2 and observed that the removal depth was nearly linear with regard to the laser fluence beyond the ablation threshold. This trend shows good agreement with those in previous studies [8,9].

4. Conclusion

Here, we demonstrated the laser decontamination of stainless steel samples using a single-mode CW laser. By repetitively exposing the single-mode CW laser to a confined region at a high scanning rate, we successfully removed the metal surface to a depth of more than 40 μm, which shows the potential to achieve an extremely high DF up to 1000 by simply increasing the number of scans.

In addition, the DF can be improved further by increasing the laser power. However, in such a case, the scan speed must be optimized to avoid any intrinsic melting. Specifically, it was found that the scan speed should exceed 10 m/s at a laser power level of 300 W to minimize thermally induced, uneven aggregation patterns under the given experimental conditions. We also observed excellent homogeneity of the surface appearance in the 10-m/s scan speed condition. Furthermore, we identified the ablation threshold value for single-mode CW laser-based decontamination.

There are several benefits when decontaminating using the single-mode CW laser. This technique removes RI contaminants from the surfaces of metals thoroughly. It also offers excellent cost-effectiveness. In addition, it can significantly reduce secondary waste from the decontamination process. The higher laser power of the single-mode CW laser system also enables faster and wider decontaminating operations. Thus, we expect that the single-mode CW laser will be an excellent solution for decontaminating primary circuits in nuclear power plants with a proper usage given its advantages.

Declaration of competing interest

The authors declare that they have no known competing financial interests or personal relationships that could have appeared to influence the work reported in this paper.

Acknowledgements

This research was supported by the Korea Atomic Energy Research Institute (KAERI) granted funding by the Korean government [Project No. 79771-21].

References

[1] J.P. Nilaya, P. Raote, A. Kumar, D.J. Biswas, Laser-assisted decontamination—a wavelength dependent study, Appl. Surf. Sci. 254 (2008) 7377–7380.
[2] Ph Delaporte, M. Gastaud, W. Marine, M. Sentis, O. Uteza, P. Thouvenot, J.L. Alcaraz, J.M. Samedy, D. Blin, Dry excimer laser cleaning applied to unclear decontamination, Appl. Surf. Sci. 208 (2003) 298–305.
[3] P.J. Maziasz, J.T. Busby, Jeremy, Properties of Austenitic Steels for Nuclear Reactor Applications, Elsevier, England, 2012, pp. 267–283.
[4] L.E. Boing, Decommissioning of nuclear facilities decontamination technologies, in: R^{2}D^{2}Project Workshop, 2006. Manila, Philippines, October 16-20.
[5] V. Kumar, R. Goel, R. Chawla, M. Silambarasan, R.K. Sharma, Chemical, biological, radiological, and nuclear decontamination: recent trends and future perspective, J. Pharm. BioAllied Sci. 2 (2010) 220–238.
[6] L. Carvalho, W. Pacquentin, M. Tabarant, A. Semerok, H. Maskrot, Metal decontamination by high repetition rate nanosecond fiber laser: application to oxidized and Eu-contaminated stainless steel, Appl. Surf. Sci. 526 (2020), 146654.
[7] A.J. Potiens Jr., J.C. Dellamano, R. Vicente, M.P. Raele, N.U. Wetter, E. Landulfo, Laser decontamination of the radioactive lightning rods, Radiat. Phys. Chem. 95 (2014) 188–190.
[8] G. Greifzu, T. Kahl, M. Herrmann, W. Lippmann, A. Hurtado, Laser-based decontamination of metal surfaces, Opt Laser. Technol. 117 (2019) 293–298.
[9] A. Kumar, T. Prakash, M. Prasad, S. Shail, R.B. Bhatt, P.G. Behere, D.J. Biswas, Laser assisted removal of fixed radioactive contamination from metallic substrate, Nucl. Eng. Des. 320 (2017) 183–186.
[10] Y. Lin, Y. Huang, A. Chiang, A compact and portable laser radioactive decontamination system using passive Q-switched fiber laser and polygon scanner, Appl. Radiat. Isot. 153 (2019), 108835.
[11] E.J. Minehara, A new laser decontamination device, Rev. Laser Eng. 40 (2011) 165–170.
[12] E.J. Minehara, K. Tamura, Laser cleaning trials for the heavily radioisotope-contaminated stainless-steel samples in the primary cooling loop of the nuclear reactor, J. RANDEC 48 (2013) 47–55.

[13] G. Guerrero-Vaca, O. Rodríguez-Alabanda, P.E. Romero, C. Soriano, E. Molero, J. Lambarri, Stripping of PFA Fluoropolymer Coatings Using a Nd:YAG Laser (Q-Switch) and an Yb Fiber Laser (CW), vol. 11, 2019, p. 1738.
[14] J. Min, H. Wan, B.E. Carlson, J. Lina, C. Suna, Application of laser ablation in adhesive bonding of metallic materials: a review, Opt Laser. Technol. 128 (2020), 106188.
[15] K.H. Leong, B.V. Hunter, J.E. Grace, M.J. Pellin, H.F. Leidich, T.R. Kugler, Laser-based Characterization and Decontamination of Contaminated Facilities, Argonne National Lab, United States, ICALEO A85, 1996.
[16] R.L. Demmer, R.L. Ferguson, Testing and Evaluation of Light Ablation Decontamination, Idaho National Engineering Laboratory, United States, INEL, 1994, 94/1034.
[17] L. Li, W.M. Steen, P.J. Modern, J.T. Spencer, Laser removal of surface and embedded contaminations on/in building structures, Lasers Mater. Process. Machin. SPIE 2246 (1994).
[18] L. Carvalho, W. Pacquentin, M. Tabarant, H. Maskrot, A. Semerok, Growth of micrometric oxide layers to explore laser decontamination of metallic surfaces, EPJ Nucl. Sci. Technol. 3 (2017) 3.